Confinement-Driven Phase Separation of Quantum Liquid Mixtures

T. R. Prisk, C. Pantalei, H. Kaiser, and P. E. Sokol

Phys. Rev. Lett. **109**, 075301 — Published 16 August 2012

DOI: 10.1103/PhysRevLett.109.075301

Confinement Driven Phase Separation of Quantum Liquid Mixtures

T.R. Prisk[1], C. Pantalei[2], H. Kaiser[1], and P.E. Sokol[1]
[1]*Indiana University, Department of Physics, Bloomington, IN 47405, USA*
[2]*École Normale Supérieure, Paris, France*

Date Submitted to *Physical Review Letters*: **June 6th, 2012**

Abstract: We report Small-Angle Neutron Scattering (SANS) studies of liquid helium mixtures confined in MCM-41, a porous silica glass with narrow cylindrical nanopores (d = 3.4 nm). MCM-41 is an ideal model adsorbent for fundamental studies of gas sorption in porous media because its monodisperse pores are arranged in a 2D triangular lattice. The small-angle scattering consists of a series of diffraction peaks whose intensities are determined by how the imbibed liquid fills the pores. Pure ^{4}He adsorbed in the pores show classic, layer-by-layer film growth as a function of pore filling, leaving the long range symmetry of the system intact. In contrast, the adsorption of ^{3}He-^{4}He mixtures produces a structure incommensurate with the pore lattice. Neither capillary condensation nor preferential adsorption of one helium isotope to the pore walls can provide the symmetry breaking mechanism. The scattering is consistent with the formation of randomly distributed liquid-liquid micro-domains ~2.3 nm in size, providing evidence that confinement in a nanometer scale capillary can drive local phase separation in quantum liquid mixtures.

Contemporary scientific interest in the behavior of binary liquid mixtures in confinement is stimulated by novel phase separation phenomena shown by these systems which do not occur in bulk systems[1]. In confinement, classical liquid mixtures do not undergo global phase separation on experimentally accessible time scales; instead, phase separation occurs by the formation of micro-domains whose characteristic length depends upon both temperature and pore diameter. The helium liquids have long been studied as model systems due to their extreme quantum nature[2]. In large pore materials like aerogel[3-5] or Vycor[6], the phase diagram of liquid ^{3}He-^{4}He mixtures shows relatively modest changes from the bulk: the unstable region breaks away from the superfluid transition line and the tricritical point disappears. The behavior of liquid helium mixtures in small pores, where confinement and interaction with the adsorbent are expected to dominate, remains largely unexplored.

We report in this Letter the results of a Small-Angle Neutron Scattering (SANS) study of liquid helium mixtures confined within MCM-41, a porous silica glass with narrow cylindrical nanopores d = 3.4 nm. The pores are arranged in a 2D triangular lattice, giving the system long range translational order. The small-angle scattering consists of diffraction peaks whose intensities are determined by how the imbibed liquid fills the pores. The well-defined pore geometry together with its regular pore array makes MCM-41 an ideal model adsorbent for fundamental studies of gas sorption in porous media.

Adsorption of ^{4}He proceeds by layer-by-layer film growth, demonstrated in the SANS data by no change in the underlying triangular symmetry of the scattering system. In contrast, when ^{3}He-^{4}He mixtures are studied, a structure incommensurate with the pore lattice is observed. This implies that symmetry along the pore axis has been broken and that the adsorbed liquid no longer forms uniform layers. The formation of randomly distributed liquid-vapor or liquid-liquid micro-domains within the pore volume would explain such an incommensurate structure, and this type of phase separation has been observed for lutidine-water mixtures in Vycor[7-9]. In the two-phase region of the bulk lutidine-water mixtures, the confined system shows slow phase separation in which the phases are segregated into domains[1]. Whereas, for ^{3}He-^{4}He mixtures infused within MCM-41, the formation of micro-domains takes place well above (by nearly a factor of 5 in temperature) the two phase region.

Mobil Corporate Material-41 (MCM-41), a templated silica glass[10-12], provided the porous matrix for these studies. An MCM-41 sample synthesized in our laboratory was characterized by small-angle X-ray scattering (SAXS) and nitrogen adsorption isotherms[13-14]. The SAXS measurements show (10) and (11) Bragg reflections at wavevector transfers of 0.17 Å^{-1} and 0.29 Å^{-1}, indicating a triangular lattice with a spacing of a = 4.25 nm. The N_2 isotherm is Type IV[15] and shows a steep capillary condensation branch, an indication of a narrow pore size distribution. The Brunauer-Emmett-Teller (BET) surface area is 740 m^2/g and total pore volume is 0.63 cc/g. The Barrett-Joyner-Halenda (BJH) pore diameter is 3.4 nm, which is consistent with the BET surface-to-volume ratio $d = 4V/A$ = 3.4 nm.

SANS measurements were carried out using the High-Flux Isotope Reactor (HFIR) at Oak Ridge National Laboratory with neutron wavelength $\lambda = 4.7$ Å, and $\delta\lambda/\lambda = 0.13$. The sample, dark current, and beam transmission were measured. The raw data was converted to $I(Q)$ using data reduction routines standard at HFIR. The low temperatures were achieved using an ILL-type orange cryostat, and gas loadings were performed *in situ*. ^{4}He was measured in the normal phase at $T = 3$ K and in the (presumed) superfluid state at $T = 1.6$ K. Mixtures with ^{3}He molar concentrations of 12% and 25% were studied at $T = 3.0$ K. The bulk phase separation temperatures for these mixtures is approximately 0.29 K and 0.54 K, respectively. Based on gas sorption isotherms[16, 17] and neutron scattering measurements[16, 18, 19], it is likely that the first layer or two of helium adsorbed on the pore walls form a solid. These amorphous solid layers are approximately 0.5 nm thick, confining the core liquid to a thin tube about 2.4 nm in diameter.

The small-angle scattering intensity $I(Q)$ from parallel, cylindrical nanopores is given by[20-22]:

$$I(Q) = \left|F(Q)\right|^2 S(Q) + G(Q) \qquad \textbf{(Eq-1)}$$

where $F(Q)$ is the form factor for the pores and adsorbed helium and $S(Q)$ is the structure factor of the porous matrix. $S(Q)$ is determined by the long range symmetry of the porous matrix while $F(Q)$ is determined by the arrangement of material within each unit cell. For the 2D triangular lattice of pores, the (hk) Bragg peak location is $Q_{(hk)} = 4\pi\sqrt{h^2 + k^2 + hk}\,/\,a\sqrt{3}$ and the delta functions $\delta(Q - Q_{(\mathrm{hk})})$ in $S(Q)$ are weighted by multiplicity factors and $1/Q^2$. $G(Q)$ is the contribution of the scattering from the MCM-41 granules (approximate size of 10 μm), which forms a sloping "background" in the Q-range of interest here. This contribution was removed by fitting the observed scattering of the empty matrix to a Harris function outside the peak regions and subtracting this from the data.

Previous measurements of ^{4}He adsorbed in nanopores have suggested layer-by-layer film growth with no capillary condensation[17]. In this case, the form factor[21] $F(Q)$ is:

$$F(Q,f) = 2\pi\rho_m R^2 \left[\alpha(1-f)\frac{J_1\left(QR\sqrt{1-f}\right)}{QR\sqrt{1-f}} + (1-\alpha)\frac{J_1(QR)}{QR}\right] \qquad \textbf{(Eq-2)}$$

where R is the pore radius, f is the volume filling fraction, and $\alpha = \rho_h/\rho_m$ is the contrast between the helium scattering length density ρ_h and that of the matrix ρ_m. J_n denotes the n^{th} Bessel function of the first kind. We note that in the case of empty pores ($f = 0$), SANS provides a direct measure of the pore radius R. Comparing the intensity of the (10) and (11) peaks yields a pore diameter in good agreement with the X-ray and isotherm results.

The ^{4}He scattering as a function of f at 3.0 K is shown in Figure 1. Nearly identical results are obtained at $T = 1.6$ K. Adsorption of ^{4}He results in a change in the intensity of the (10) and (11)

peaks with no change in either their location or shape. The (10) and (11) peaks at $f = 0$ are each well fit by a sum of two Gaussians. The solids lines in the figure represent this fit, scaled by a factor s, to match the area of the peaks with ^{4}He present. The excellent agreement between the shape and position of these scaled peaks is an unambiguous indication that ^{4}He is adsorbing in layers along the pore surface and that these layers do not alter the underlying long range symmetry of the pore structure. This is illustrated schematically in the inset of Figure 1. The variation of the scaling factor s with pore filling is shown in Figure 2. Equation 2 was fit to the data by varying the density of the adsorbed liquid and α, which depends strongly on –OH groups and other impurities from the synthesis process. The agreement is excellent, supporting layer-by-layer film growth.

The behavior upon adsorption of helium mixtures, shown in Figures 3 and 4, is strikingly different from the pure ^{4}He case. At low fillings, the peaks appear to have the same position and shape as for the empty porous matrix but with intensities that are not predicted by the uniform film behavior used in Equation 2. At higher fillings, the scattering cannot be described by simply scaling the peaks that are observed for the empty pores. New scattering, not present in the pure ^{4}He case, is clearly present between the (10) and (11) peaks. This represents a clear breakdown of the assumption used to derive Equation 1 that the film retains the same symmetry as the pores. To reinforce this point, the solid lines in Figures 3 and 4 show the predication of Equation 2 accounting for the different molar volume and neutron scattering length density of the mixtures. The scattering that appears at high filling is not consistent with the 2D symmetry of the matrix.

It should be emphasized that preferential adsorption of one isotope of helium to the pore walls does not break symmetry along the pore axis. Previous studies have suggested that ^{4}He is preferentially adsorbed on the pore walls, leaving ^{3}He-rich liquid in the core volume of the pores[5]. However, such preferential adsorption would not break the underlying symmetry and Equation 1 would still remain valid, although a more sophisticated $F(Q)$ reflecting the density variation of the film would be required. The breakdown of Equation 1 is a clear indication of the formation of a structure *incommensurate with the pore lattice*.

It might be thought that capillary condensation provides the symmetry-breaking mechanism. There are two reasons to doubt this explanation of the symmetry breaking. First, the additional broad feature between the (10) and (11) Bragg peaks will disappear at high fillings as the underling symmetry of the lattice is restored. Instead, we find that it continues to grow in intensity as further mixture is adsorbed. Second, capillary condensation will be visible in the scattering only if it occurs on the length scales accessible to the spectrometer. Thus, the capillary will only affect the symmetry when it is in the 1-100 nm range and would be seen as a feature moving to lower Q as the necks grow and disappearing into the low Q background. This is inconsistent with the observed behavior. Other mechanisms beside capillary condensation are required to describe the appearance of an incommensurate structure.

The formation of randomly distributed liquid-vapor or liquid-liquid micro-domains within the pore volume would explain the symmetry breaking. This is illustrated by the inset cartoon in Figure 3. The peak maximum, which occurs around 0.27 $Å^{-1}$, corresponds to a characteristic length scale of roughly 2.3 nm. There is sufficient contrast in scattering length density (SLD) to observe the formation of ^{3}He-rich droplets within the core volume of the pores. The coherent SLD of bulk liquid ^{3}He is 32% greater than bulk liquid ^{4}He. Local phase separation or domain formation of this kind has been observed for classical liquids in other porous media[1,7], the difference here being that the separation is occurring significantly above the bulk critical temperature $T > T_c$. For the helium mixtures we studied, phase separation occurs for bulk mixtures below 0.6 K, whereas we observe these effects at 3 K.

This behavior seems inconsistent with the theoretical treatments of confined binary mixtures in the literature[8-9, 23-29]. These models do not, to our knowledge, predict the formation of these kinds of structures at $T >> T_c$. Liu *et al* claim that it is possible for bubbles of vapor to become trapped in liquid during capillary condensation[8]. Imre points out that applying even a small *negative* pressure to a ^{3}He-^{4}He mixture brings the liquid close to the spinodal point of ^{3}He. This will cause mixtures in nanopores to undergo phase separation at temperatures where the bulk mixture is homogenous[30]. Gelb *et al* emphasize that true thermodynamic phase transitions cannot occur in one-dimension, and that this complicates the analysis of phase separation in cylindrical pores[1]. They emphasize that no real critical behavior is observed in cylindrical pore systems because correlations can grow large only in one direction. For the core liquid in our system, ratio of atomic diameter to pore diameter is $d_{He}/d_{core} \approx 0.11$. It is conceivable that dimensional reduction plays an important role in the anomalous structure reported here. New ideas are needed to understand the novel formation of microdomains at temperatures much higher than T_c in quantum liquid systems.

In this Letter, we reported the results of a SANS study of liquid helium mixtures infused within a porous silica glass, MCM-41, which has cylindrical nanopores with a diameter of 3.4 nm. The adsorption of ^{4}He occurs by layer-by-layer film growth along the pore walls. Because the helium film does not change the underlying long range symmetry of the pore structure, this results in changes to the intensity of the (*hk*) diffraction peaks with no change in either their location or shape. When isotopic mixtures are adsorbed within the porous host, a structure incommensurate is observed in the scattering data which implies that symmetry along the pore axis has been broken. This is evidence that confinement induces phase separation in quantum liquid mixtures.

This report was prepared at Indiana University under award 70NANB5H1163 from the National Institute of Standards and Technology, U.S. Department of Commerce. The statements, findings, conclusions, and recommendations are those of the authors and do not necessarily reflect the views of the National Institute of Standards and Technology or the U.S. Department of Commerce. This research at Oak Ridge National Laboratory's High Flux Isotope Reactor was sponsored by the Scientific User Facilities Division, Office of Basic Energy Sciences, U.S. Department of Energy. The authors wish to thank Yuri Melnichenko, Ken Litrell, and David

Sprinkle for their expert assistance. The authors are indebted to Michihiro Nagao, Christopher Stock, Emilio Cobanera, and Matthew Bryan for stimulating conversation and criticism.

References

[1] L.D. Gelb, K.E. Gubbins, R. Radhakrishnan, M. Sliwinska-Bartkowiak, *Rep. Prog. Phys.* **62**, 1573-1659 (1999)
[2] E.G. D. Cohen, *Science* **197**, no. 4298, 11-16 (1977)
[3] S.B. Kim, J. Ma, M.H.W. Chan, *Phys. Rev. Lett.* **71**, 2268-2271 **(**1993)
[4] N. Mulders and M. H.W. Chan, *Phys. Rev. Lett*. **75**, 3705 (1995).
[5] L. B. Lurio, N. Mulders, M. Paetkau, M.H.W. Chan, S.G.J. Mochrie, *Phys. Rev. E* **76**, 011506 (2007)
[6] Th. Hohenberger, R. König, and F. Pobell, *JLTP*, **110**, 579-584 (1998)
[7] M. Y. Lin, S. K. Sinha, J. M. Drake, W. Wu, P. Thiyagarajan, and H. B. Stanley, *Phys. Rev. Lett.* **72** 2207-2210 (1994)
[8] A. J. Liu, D. J. Durian, E. Herbolzheimer, and S. A. Safran, *Phys. Rev. Lett.* **65**, 1897 (1990)
[9] A. J. Liu and G.S. Crest, *Phys. Rev A* **44**, R7894 (1991)
[10] J.S. Beck, J.C. Vartuli, W.J. Roth, M.E. Leonowicz, C.T. Kresge, K.D. Schmitt, C.T-W. Chu, D.H. Olson, E.W. Shappard, S.B. McCullen, J.B. Higgins, and J.L. Schlenker, *J. Am. Chem. Soc.* **114**, 10834-10843 (1992)
[11] M. Grün, I. Lauer, K.K. Unger, *Adv. Mater.* **9**, 254 (1997)
[12] X.S. Zhao, G.Q. Lu, G. J. Millar, *Ind. Eng. Chem. Res.* **35**, 2075-2090 (1996)
[13] D.D. Duong, *Adsorption Analysis: Equilibria and Kinetics*, Imperial College Press (1998)
[14] S. J. Greg and K.S.W. Sing, *Adsorption, Surface Area, and Porosity*, Academic Press (1967)
[15] K.S.W. Sing, D.H. Everett, R.A.W. Haul, L. Moscou, R.A. Pierotti, J. Rouquérol, T. Siemieniewska, *Pure Appl. Chem.*, **157,** 603-619 (1985)
[16] F. Albergamo, J. Bossy, H.R. Glyde, A. J. Dianoux, *Phys. Rev. B* **67**, 224506 (2003)
[17] H. Ikegami, T. Okuno, Y. Yamoto, J. Taniguchi, N. Wada, S. Inagaki, and Y. Fushima, *Phys. Rev B*, **68**, 092501 (2003)
[18] C.R. Anderson, K.H. Andersen, W.G. Stirling, P.E. Sokol, and R. M. Dimeo, *Phys. Rev. B*, **65**, 174509 (2002)
[19] C. Andreani, C. Pantalei, and R. Senesi, *Phys. Rev. B*, **75**, 064515 (2007)
[20] M. Engel, B. Stühn, J. J. Schneider, T. Cornelius, M. Naumann, *Appl Phys A* **97**, 99-108 (2009)
[21] A. Schreiber, I. Ketelsen, G.H. Findenegg, and E. Hoinkis, *Studies in Surface Science and Catalysis* **160**, 17-24 (2007)
[22] K. J. Edler, P.A. Reynolds, J.W. White, D. Cookson, *J. Chem. Soc. Faraday. Trans.* **93** (1),

199-202 (1997)
[23] M. Impéror-Cler, P. Davidson, A. Davidson, *J. Amer. Chem. Soc* **122** 11925 (2000)
[24] O. Glatter and O. Kratky, *Small-Angle X-ray Scattering*, Academic Press, London (1982)
[25] P. G. de Gennes, *J. Phys. Chem.* **88**, 6469 (1984)
[26] F. Brochard and P.G. de Gennes, *J. Phys. Lett.* **44**, 785 (1983)
[27] M. Blume, V. J. Emery, and R. B. Griffiths, *Phys. Rev. A* **4**, 1071 (1971)
[28] A. Maritan, M. Cieplak, M.R. Swift, F. Toigo, J. R. Banavar, *Phys. Rev. Lett.* **69**, 221-224 (1992)
[29] L. Pricaupenko and J. Treiner, *Phys. Rev. Lett.* **74**, 430 (1995)
[30] A.R. Imre, H.J. Maris, and P.R. Williams, *Liquids Under Negative Pressure*, Kluwer Academic Publishers (2002)

Figures

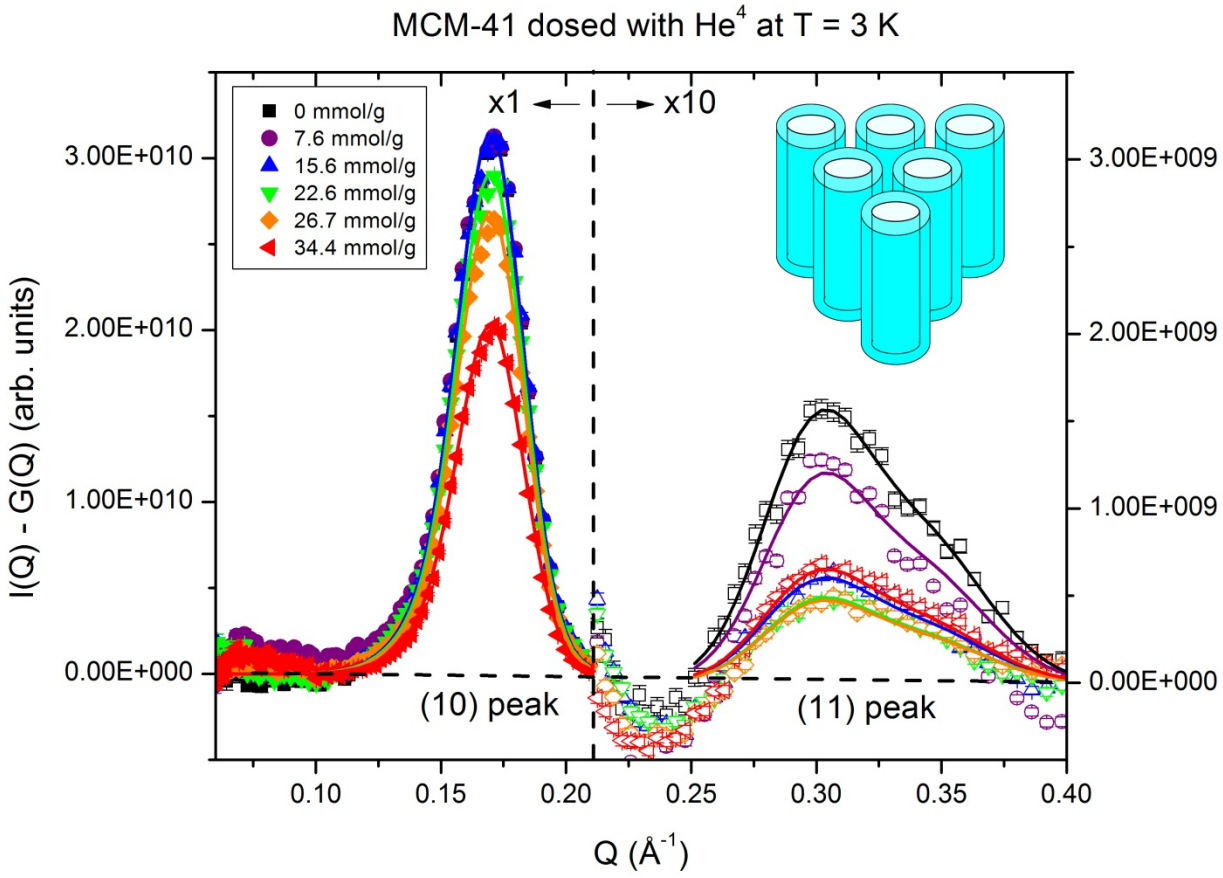

Figure 1. The modulation of (*hk*) peak intensity when MCM-41 is dosed with ^{4}He at T = 3.0 K. The open symbols have been scaled by a factor of 10 for clarity and use the right hand vertical axis.

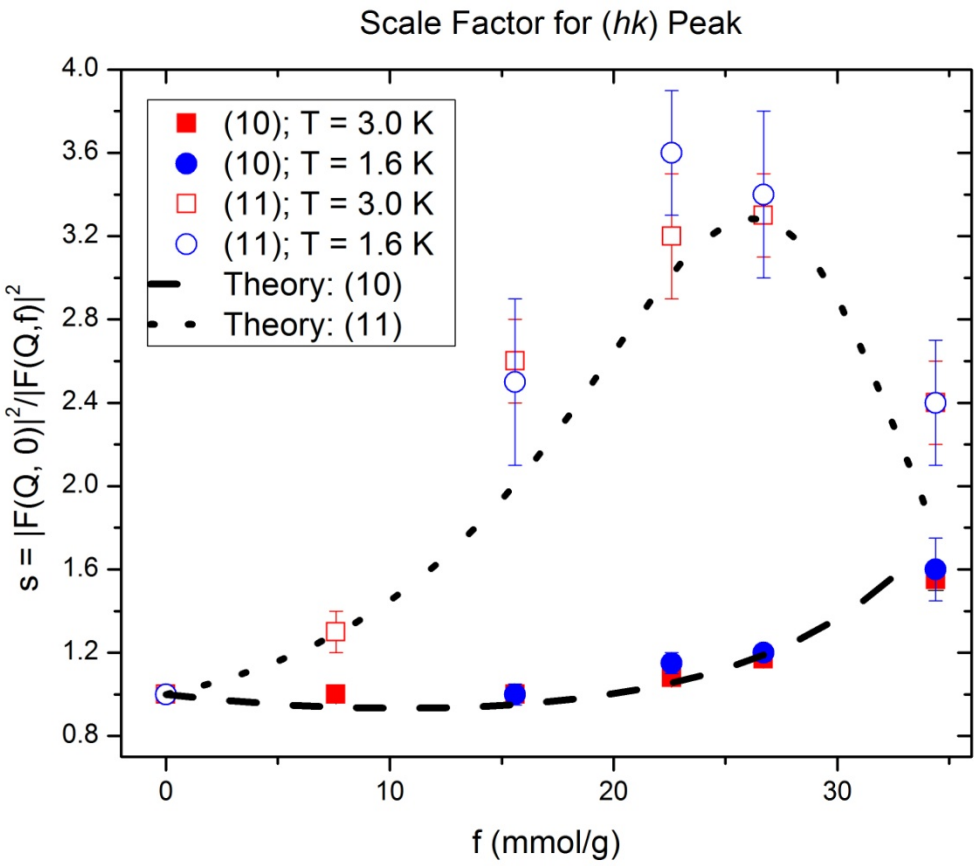

Figure 2. The measured values of $s = |F(f = 0, Q)|^2/|F(f, Q)|^2$ with filling f, for the (10) and (11) peaks. The lines are the predictions of Equation 2.

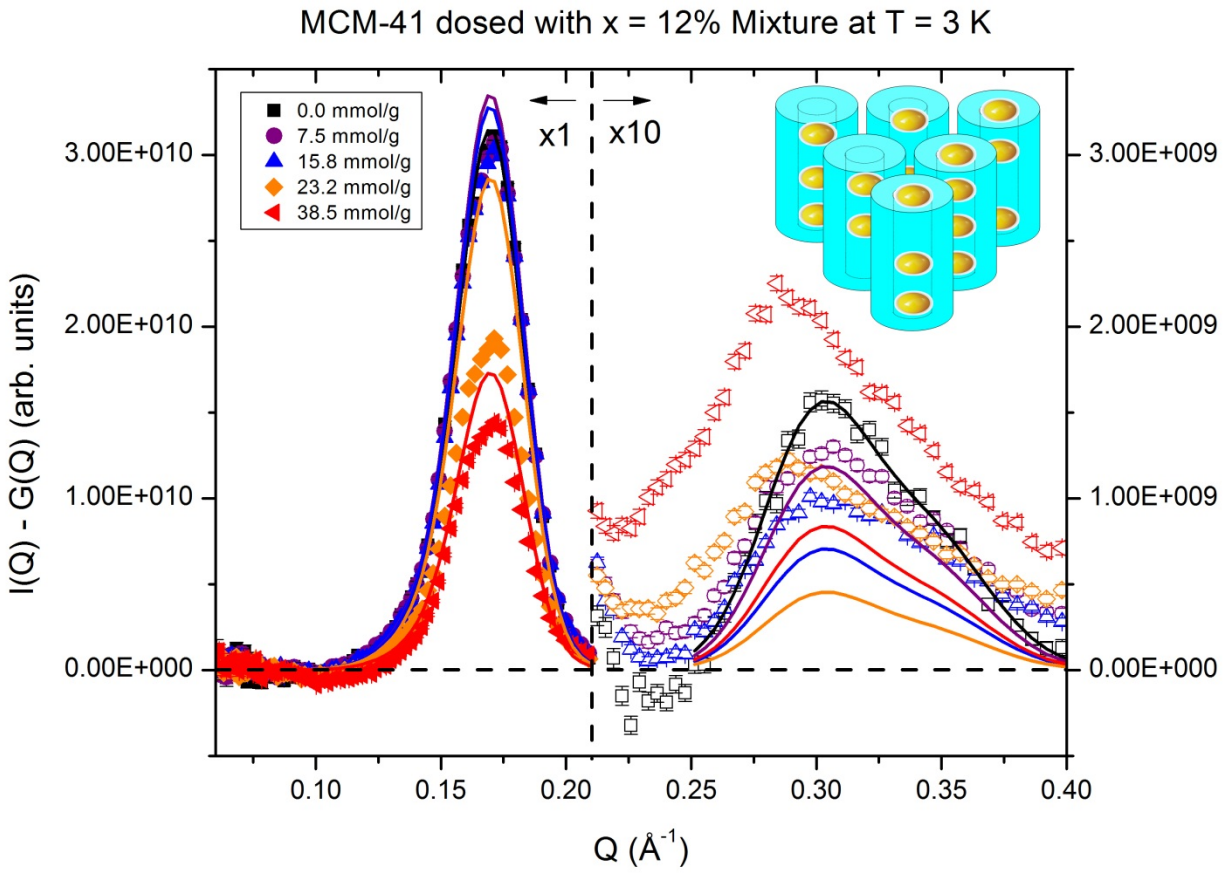

Figure 3. The modulation of (*hk*) peak intensity when MCM-41 is dosed a x = 0.12 helium mixture at T = 3.0 K. The open symbols have been scaled by a factor of 10 for clarity and use the right hand vertical axis. The solid lines are expected behavior based on a film growth model. The deviations from the model predictions are clearly evident.

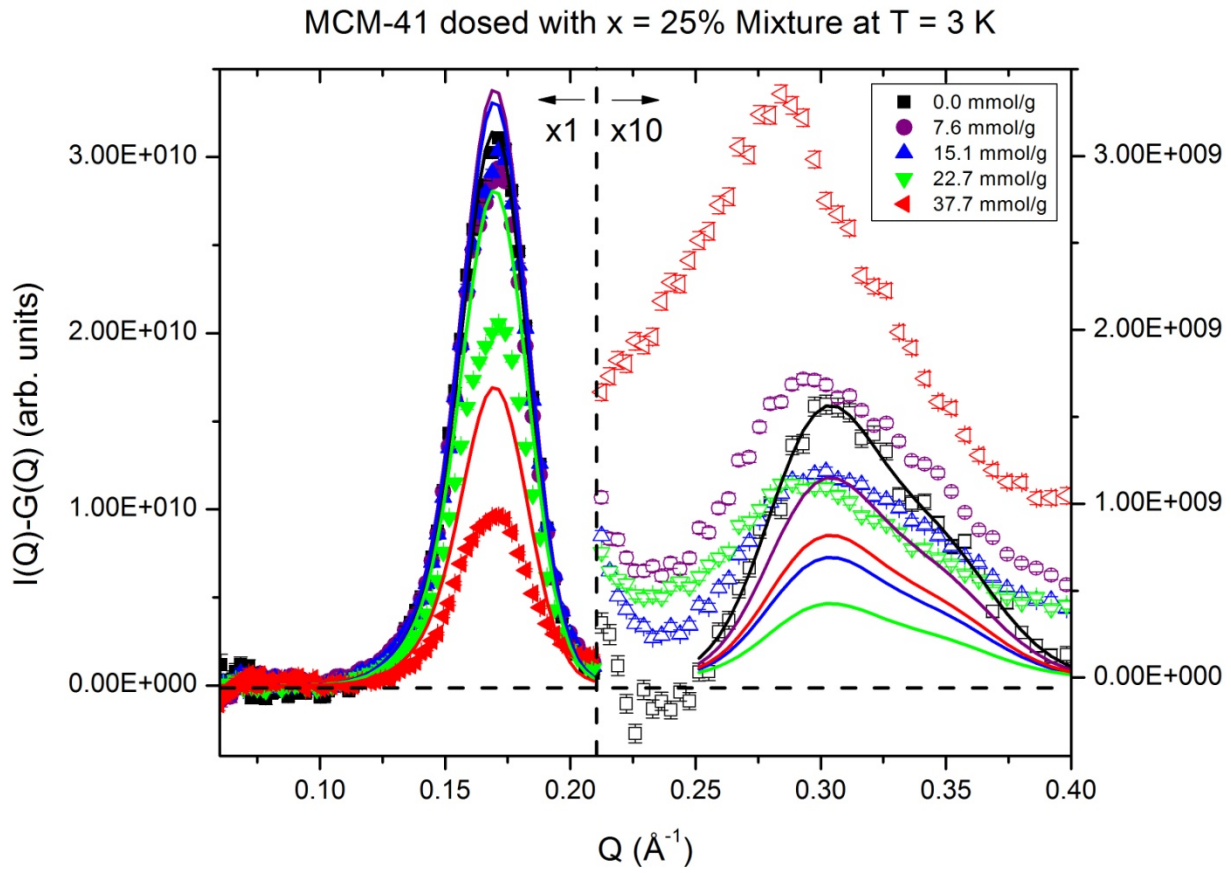

Figure 4. The modulation of (*hk*) peak intensity when MCM-41 is dosed a $x = 0.25$ helium mixture at $T = 3.0$ K. The open symbols have been scaled by a factor of 10 for clarity and use the right hand vertical axis. The solid lines are expected behavior based on a film growth model. The deviations from the model predictions are pronounced.